



STUDY OF THE TRANSPORT PROPERTIES OF POLYCRYSTALLINE DOLOMITE ($\text{CaMg}(\text{CO}_3)_2$) BY THE THERMALLY STIMULATED DEPolarIZATION CURRENT TECHNIQUE

A. N. PAPATHANASSIOU and J. GRAMMATIKAKIS

University of Athens, Department of Physics, Section of Solid State Physics, Panepistimiopolis, GR 157 84 Zografos, Athens, Greece

(Received 4 September 1996; accepted 2 December 1996)

Abstract—The thermally stimulated depolarization current (TSDC) technique is employed to study the transport phenomena in dolomite which is unstable at high temperatures. The spectrum of polycrystalline dolomite exhibits a strong relaxation peak which reaches a maximum close to room temperature. The dependence of the data on the polarization conditions, the electrode material and the sample thickness suggests that the mechanism responsible for the TSDC peak is related to space charge relaxation and that the polarization of the material is inhomogeneous, involving long distance free charge migration. A selective polarization mode was applied in order to sample the response components, while the partial heating technique led to a temperature distribution of activation energy values. © 1997 Elsevier Science Ltd. All rights reserved.

Keywords: A. polycrystalline materials, C. ionic thermocurrent, D. dielectric properties, D. electrical properties, D. transport properties.

INTRODUCTION

Dolomite ($\text{CaMg}(\text{CO}_3)_2$ or $\text{CaCO}_3:\text{MgCO}_3$), calcite (CaCO_3) and magnesite (MgCO_3) constitute the so-called 'calcite family' and share a rhombohedral crystal structure [1, 2]. They are typical representatives of the alkaline earth carbonate salts and have recently attracted the interest of pure and applied research groups [3–5]. The present paper presents a portion of our work on the calcite family materials and some results emphasizing the dielectric and transport properties under pressure that have recently appeared elsewhere [5–9]. The interest in experimental study stems from the necessity to investigate ionic systems more complicated than those studied during the few last decades (mainly alkali halides and alkaline earth fluorides [10]). Additionally, the calcite family is a group of ionic crystals 'proper' for relating the physical properties of the mixed ionic crystal (dolomite) in terms of its end members' (calcite and magnesite) properties. As the calcite family members are widespread industrial materials, the research may provide valuable information for improving and extending their industrial use. Finally, further insight into their physical properties is expected to contribute to our understanding of large scale physical phenomena that develop in the earth's crust, since carbonate salts manifest themselves as important geomaterials.

The transport properties of ionic materials are usually studied by performing conductivity and/or

diffusion measurements at different temperatures [11, 12]. The ionic conductivity σ depends exponentially upon the inverse of temperature according to the following formula [12]:

$$\sigma(T) = \frac{\sigma_0}{T} \exp\left[-\frac{E}{kT}\right], \quad (1)$$

where k is the Boltzmann's constant, E denotes the activation energy and σ_0 is the pre-exponential factor that involves the concentration of charge carriers, the vibrating frequency of the moving species and some geometrical factors, and is assumed to be practically constant. For an ionic crystal, the temperature region where defects created by incorporation of aliovalent impurities (i.e. extrinsic vacancies) are unassociated to the impurity ions is called the 'extrinsic unassociated' region, and the activation energy E that appears in eqn (1) is identical to the migration enthalpy h^m of the free carriers [13, 14]. Therefore, measurement of the ionic conductivity in the extrinsic unassociated region (usually at some hundreds of degrees above the room temperature (RT)) can lead to the evaluation of the very important migration enthalpy h^m for the migration of free charge carriers. The migration enthalpy is directly related to the height of the potential barrier that the moving ion jumps in travelling from one equilibrium to a neighbouring one.

From another viewpoint, the transport phenomena can also be probed by dielectric relaxation experiments, in

which polarization of an ionic solid is due to the rotation of dipoles and the hopping migration of free charge carriers. Under the application of an external electric field, the dipoles can orientate while the free charge carriers travel along the sample, contributing to the d.c. conductivity unless some boundary conditions prohibit their motion towards the electrodes [15]. Internal boundaries (grain boundaries, dislocations etc.) result in localized polarization, well known as Maxwell–Wagner polarization. On the other hand, the non-ohmic character of the sample–electrode interface prevents some of the free carriers from neutralizing on the electrodes, leading to formation of a space charge [16]. Either impedance measurements or polarization–depolarization measurements can, in principle, detect the free charge motion and lead to an evaluation of the migration enthalpy h^m of the free carriers [17].

Dolomite is an ionic system which is unstable at relatively low temperatures. It has been observed that at about 500–600°C the material is thermally decomposed leading to oxide formation [18, 19]. This aspect prevents us from performing conductivity measurements by increasing the temperature, in trying to work in the extrinsic unassociated region. As mentioned in the preceding paragraph, an alternative way to study the transport phenomena is to employ the thermally stimulated depolarization current (TSDC) method [20], which is a high-resolution dielectric relaxation spectroscopy method that operates at relatively low temperatures (usually from the liquid nitrogen temperature (LNT) to the vicinity of RT), and can detect the dipole relaxation and the space charge relaxation. Apart from the dielectric characterization, we may accurately obtain the energy parameters for each mechanism, i.e. the activation energy for dipole rotation or the activation energy for free charge migration. Notice that these quantities (although labelled by the same symbol) are different, as the first refers to the motion of bound defects around an impurity, while the latter refers to the motion of free (unassociated) ionic defects. In the present paper we deal with the latter case. Our work does not merely contribute to an understanding of ionic relaxation in dolomite, but serves as an alternative proposal for studying the transport phenomena in materials that are unstable at the experimental conditions under which usual conductivity measurements are carried out.

THEORY

The basic steps of the TSDC method are given here in brief [16, 21]. At temperature T_p (usually room

temperature, RT) an electric field is applied to the dielectric for the time interval t_p , which is usually much longer than the relaxation time $\tau(T_p)$ of each relaxation mechanism. The accumulation of free charges towards the sample's surfaces results in the polarization of the material. By keeping the electric field on, the sample is cooled to LNT. Since the relaxation time $\tau(\text{LNT})$ at LNT is practically infinite, the polarization state attained during the polarizing stage remains frozen, even when switching off the field. Subsequently, by heating the sample in the absence of the external field, the space charge polarization is annihilated at relatively high temperature (usually around RT) where the thermal energy is high enough to assist the spatial redistribution of the space charge. A sensitive electrometer connected to the sample surfaces during the heating procedure records a transient thermal depolarization current $I(T)$ originating from the time variation of the space charge polarization, which is described by an equation similar to the glow-like signal $I_{\text{dip}}(T)$ of rotating dipoles [22]:

$$I_{\text{dip}}(T) = \frac{S\Pi_0}{\tau_0} \exp \left[-\frac{E}{kT} - \frac{1}{b\tau_0} \int_{T_0}^T \exp\left(-\frac{E}{kT}\right) dT \right], \quad (2)$$

where Π_0 is the initial polarization of the dielectric, S is the surface sample area in contact with the electrode, E is the activation energy of the rotating dipoles (identical to the migration enthalpy h^m of the bound migrating defect), b is the constant heating rate, k is Boltzmann's constant, T_0 coincides with LNT and τ_0 is the pre-exponential factor of the usual Arrhenius law, providing the temperature dependence of the relaxation time $\tau(T)$:

$$\tau(T) = \tau_0 \exp\left(\frac{E}{kT}\right). \quad (3)$$

The space charge peaks are sensitive to the electrode material used and the blocking degree of the sample–electrode interface. The polarization state achieved strongly depends upon the storage conditions and the electret's prehistory. Only very rough approximations have been made and several space charge TSDC equations have been derived [16, 21, 23]. The common point of the different approximations is that the initial rise of the TSDC curve coincides with that of the non-interacting rotating dipoles. An expression for the initial rise can be derived directly from eqn (2) by noting that in the region of the initial rise $T \approx T_0$ and, therefore, the integral in eqn (2) is zero. Thus, for the initial rise region we

may write:

$$I(T) \propto \exp\left(-\frac{E}{kT}\right), \quad (4)$$

where I denotes the depolarization current, k the Boltzmann's constant and E the activation energy for the diffusion of free ionic charge carriers, which coincides with the migration enthalpy h^m of the free migrating entities and is a different quantity from the activation energy of the dipolar reorientation. Subsequently, the evaluation of the activation energy E can be attained, whatever model is assumed to describe the depolarization phenomenon.

EXPERIMENTAL DETAILS

The temperature range of our cryostat is from LNT to 400 K. An Alcatel molecular vacuum pump was used to create a pressure better than 10^{-6} mbar. The crystals were placed between the platinum electrodes and were polarized using a Keithley 246 d.c. power supply. The temperature was measured by means of a gold-chromel thermocouple fed into the upper electrode, which was connected to an Air Products temperature controller. The temperature rise at a constant rate (ranging from 3.0 to 3.5 K min⁻¹) was monitored by the controller and the desired (constant) heating rate was maintained throughout each TSDC scan. The depolarization current was measured with a Cary 401 electrometer. Currents of the order of 10^{-16} A could be detected. The output signals from the controller and the electrometer were digitized via a Keithley DAS 8 PGA card installed into a computer. The data were afterwards analysed with appropriate software.

The material we studied is natural polycrystalline, greyish, compact rock dolomite from Greece. It is used in industrial applications and was accompanied by the chemical analysis results from Cimprogetti SPA Laboratories, Italy: loss on ignition, 46.91 wt%; SiO₂, 0.20 wt%; Al₂O₃, 0.12 wt%; Fe₂O₃, 0.04 wt%; CaO, 30.51 wt%; MgO, 21.81 wt%. Additional analysis (Institute of Geological and Mining Research, Greece) gave: Mn, 0.02 wt%; Sr, 0.02 wt%; K, <0.01 wt%; Na, 0.01 wt%; humidity, 0.13 wt%.

RESULTS AND DISCUSSION

Dielectric characterization

The thermal depolarization spectrum of polycrystalline dolomite exhibits three relaxation mechanisms (Fig. 1), labelled LT1, LT2 and HT, which maximize at 140 K, 188 K and close to RT, respectively. The low temperature dispersions (LT1 and LT2) have previously been studied and attributed to the rotation

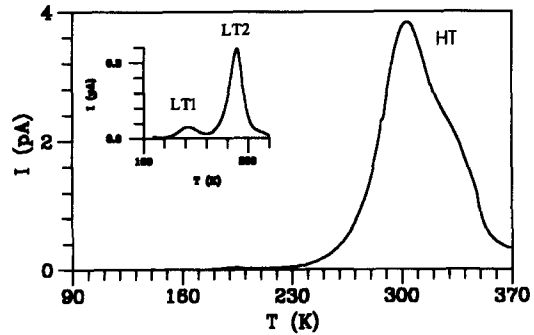


Fig. 1. Thermogram of polycrystalline dolomite. The polarizing conditions were: $T_p = 292$ K, $E_p = 7.09$ kV cm⁻¹, $t_p = 2$ min. The figure inset depicts the low temperature spectrum recorded when the polarization temperature T_p is selected so as not to have the HT mechanism polarized ($T_p = 200$ K) (see ref. [8]).

of defect dipoles [8]. In the present work, our interest is focused on the properties and the characteristics of the HT band, with the aim of understanding the depolarization and transport phenomena in the dolomite structure.

In Fig. 2 we present the HT recordings using different kinds of electrodes (platinum, bronze, graphite paint and teflon). The shape, temperature T_{max} where the peak becomes of maximum, and the charge Q released during the depolarization stage depend upon the nature of the electrodes. The maximum temperature T_{max} is located at the temperature region from 290 to 320 K when the polarization temperature T_p coincides with RT. In Table 1 we give the total polarization Π_o (a direct function of the area under the TSDC curve) detected during the thermal depolarization stage, reduced with respect to the external field intensity E_p . The variation of the Π_o/E_p ratio indicates that the mechanism is sensitive to the blocking degree and the work function of the electrode material and establishes that the HT band is a space charge one [16]. For each electrode set-up we performed three successive

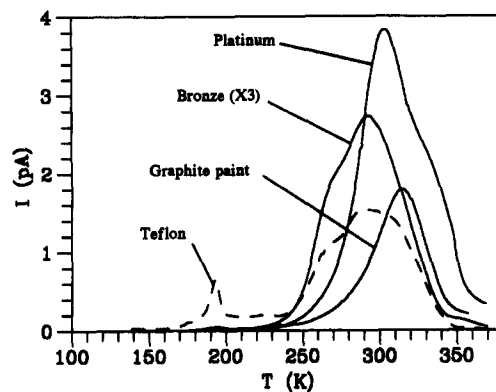


Fig. 2. Dependence of HT band of polycrystalline dolomite on the nature of the electrodes used. The polarizing conditions were: $T_p = 292$ K, $t_p = 5$ min, $E_p = 7.13$ kV cm⁻¹ (metal electrodes) and 5.99 kV cm⁻¹ (teflon electrodes).

Table 1. Dependence of polarization Π_0 , as recorded by TSDC scans, reduced with respect to electric field intensity E_p , upon electrode material used

Electrode material	$\frac{\Pi_0}{E_p} (10^{-14} \frac{C}{V \cdot mm})$
Platinum	8.26
Bronze	14.80
Graphite paint	14.87
Teflon	3.88

scans under exactly the same polarizing conditions (Fig. 3). The recordings were unreproducible and, by using metal electrodes, the end part of the curve did not reach zero. In particular, the employment of bronze electrodes often led to signal reversals at the end (i.e. at the high temperature part of the band), indicating that some injection phenomena might exist. The above-mentioned results are definitely typical of space charge relaxation. Further detailed dielectric characterization demands resolution of the HT peak into its constituents and an investigation of whether any dipolar mechanism is activated at the high temperature region and is therefore masked by the space charge processes.

As the polarization temperature T_p is reduced, the peak's maximum temperature T_{max} is lowered with a simultaneous reduction of the signal amplitude (Fig. 4). This can be interpreted in terms of a distribution in the

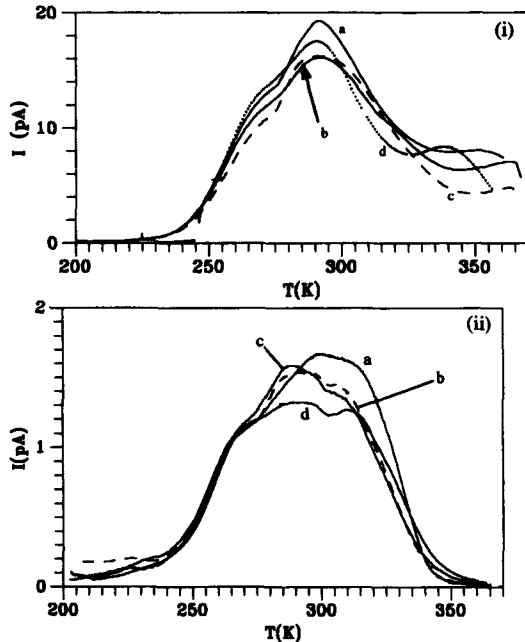


Fig. 3. Successive TSDC experiments (a, b, c and d) under exactly the same polarizing conditions using (i) metal electrodes and (ii) teflon (insulating) electrodes. The polarization conditions were: $T_p = 292$ K, $t_p = 2$ min, while the internal field intensity was $E_p = 7.43$ kV cm $^{-1}$ when platinum electrodes were used and $E_p = 5.99$ kV cm $^{-1}$ when teflon electrodes were employed.

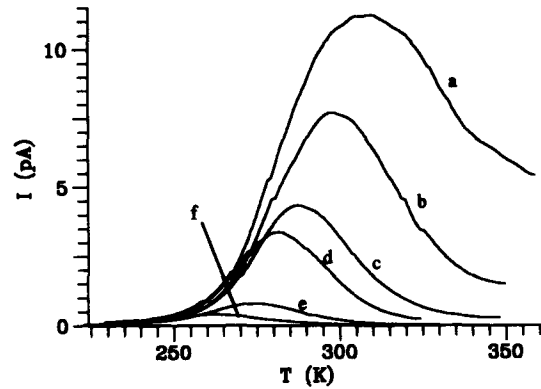


Fig. 4. Recordings of HT band as the polarization temperature T_p changes: (a) 310 K, (b) 290 K, (c) 270 K, (d) 260 K, (e) 250 K, (f) 240 K. The polarizing conditions were $E_p = 21.43$ kV cm $^{-1}$ and $t_p = 2$ min, and platinum electrodes were used.

values of the relaxation time. When T_p is larger than RT, the peak becomes quite broad and complex. The same situation is observed when insulating (teflon) electrodes are used in the MISIM (metal-insulator-sample-insulator-metal) configuration. An increase in the polarization time t_p does not lead to saturation polarization (Fig. 5) in a manner typical of space charge polarization. We did not perform experiments involving varying the intensity E_p of the polarizing electric field, due to the unreproducible nature of the space charge peak.

Keeping the polarizing conditions (T_p , t_p , E_p) constant we performed a scan on a 1.0 mm thick sample and one more scan after reduction of the sample thickness to 0.60 mm. Two polarizing temperatures were selected: $T_p = 250$ K and $T_p = 270$ K. The first was the lowest that could achieve a minimum detectable polarizable state of the mechanism and avoid the complex high temperature tails. The latter ($T_p = 270$ K) was selected in the usual manner, being close to RT. The results are the same in both cases: on decreasing the sample thickness, T_{max} is shifted and the amplitude I_{max} increases (Fig. 6). The thickness dependence

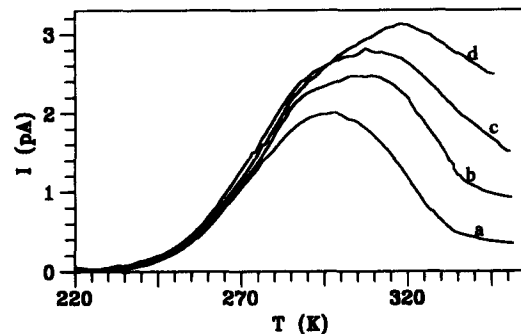


Fig. 5. Thermograms obtained by varying the polarization time t_p : (a) 2 min, (b) 5 min, (c) 10 min, (d) 20 min. The polarization temperature was $T_p = 300$ K and the electric field intensity was $E_p = 7.14$ kV cm $^{-1}$.

proves that the HT band is related to the inhomogeneous polarization of the sample [24]. This aspect is typical for space charge polarization. Supposing that reduction of the sample thickness makes the path towards the electrodes shorter, a decrease of T_{\max} would be expected, while the reduction in charge population would weaken I_{\max} [16]. Our experiments show that this oversimplified model, which ignores both the sample–electrode interface quality and the migration path topology, does not apply in dolomite. Additionally, in order to ensure that the sample microstructure remains invariant, we performed the experiments by gradually reducing the thickness of the same sample. As a consequence, the removal of slices during sample thickness reduction removes, at the same time, some of the space charge stored during previous experiments. The perturbation of the spatial space charge distribution is probably responsible for the discrepancy between our results and the model mentioned above. We stress that, whatever model we use, the thickness dependence proves that the HT peak originates from inhomogeneous polarization.

Selective polarization technique

Resolution of the HT band into its constituents relaxation mechanisms was achieved by applying the selective polarization technique [25], which is an alternative to thermal sampling [26–28], and was first applied to ionic crystals by the present authors [10]. With the aim of decomposing a complex band into its constituents, we applied the following steps. At temperature T_{pd} , which is selected from within the temperature region where the mechanism is activated, we polarize for the time interval t_p , and afterwards we short-circuit the sample, by keeping the temperature constant, for the time interval t_d . Then, the specimen is immediately cooled to LNT in order to freeze the polarization state achieved during the combined polarization–depolarization procedure.

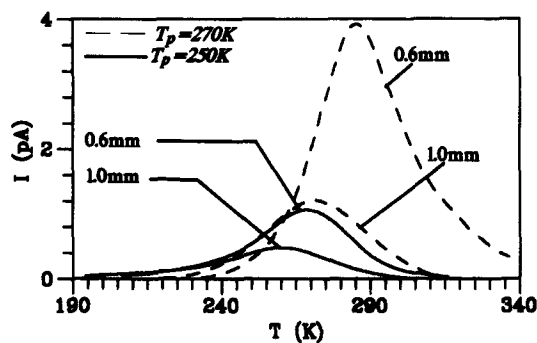


Fig. 6. Dependence of signal upon the sample thickness. The polarization conditions were: $E_p = 22.17 \text{ kV cm}^{-1}$, $t_p = 2 \text{ min}$, $T_p = 270 \text{ K}$ (dashed line) and 250 K (solid line). Thickness values are displayed in the graph.

The physical content of the aforementioned procedure is as follows. On polarizing at T_{pd} the slow relaxation mechanisms (that are activated at much higher temperature than T_{pd}) remain unpolarized, while the mechanisms activated close to T_{pd} , as well as those activated at temperatures lower than T_{pd} , reach a polarization state. On depolarizing (at T_{pd}) the low temperature polarization is destroyed as the low temperature mechanisms are much faster than those activated in the vicinity of T_{pd} . The final cooling to LNT maintains the polarization state of the mechanisms that are activated close to T_{pd} and survived the combined polarization–depolarization stage in a frozen state. By subsequent heating of the sample, a component of the initial complex band is recorded as a result of time decay of the polarization that was initially frozen. The operation is repeated by selecting different values of the T_{pd} temperatures and consequently sampling the relaxation mechanism.

By employing the selective polarization technique we probe a portion of the mechanism around the T_{pd} region and the polarization state attained depends upon the relation of the relaxation time to the polarizing time interval t_p and the discharging period t_d [25]. If T_{\max} denotes, in the usual manner, the temperature where a component reaches a maximum, a $T_{\max}(T_{pd})$ diagram provides the following valuable information: the random scatter of experimental points proves the space charge origin of the mechanism, while their fit to a straight line with a slope of unity indicates that the relaxation time distribution is a feature of the mechanism [25]. A single mechanism gives responses with maximum temperature T_{\max} independent of T_{pd} . Finally, the high reproducibility of the component peaks is typical of a dipole contribution, while space charge components suffer from unreproducibility. It is worth noticing that the variation of T_{\max} with T_{pd} is, in some respects, similar to the $T_m - T_{\text{stop}}$ procedure developed for thermoluminescence analysis [29, 30].

In our experiments we chose $t_p = t_d = 2 \text{ min}$. A representative specimen of the selective polarization responses is depicted in Fig. 7. In Fig. 8 we have drawn the maximum temperature T_{\max} and the signal amplitude I_{\max} for the complete set of component peaks detected. As T_{\max} depends on T_{pd} , we conclude that the HT band is characterized by the distribution in relaxation time. The points can hardly be fitted to a straight line, especially those located above 290 K , so we may state that the dispersion has space charge features; an aspect strongly supported by the low reproducibility of the components. As shown in Fig. 8, the signal amplitude increases on augmenting T_{pd} and, after reaching a maximum value, it decreases. Therefore, the HT band is a unique mechanism and not the

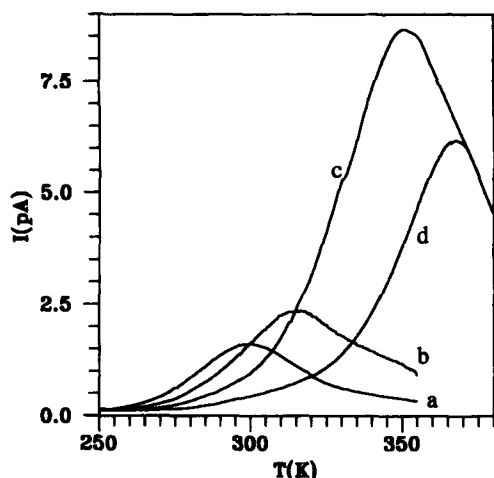


Fig. 7. A sample of the responses that build up the HT mechanism, obtained by performing the selective polarization method. The experimental conditions were: $E_p = 21.43 \text{ kV cm}^{-1}$, $t_{pd} = 2 \text{ min}$ and $T_{pd} = 280 \text{ K}$ (a), 290 K (b), 320 K (c), 357 K (d).

overlapping of two (or more) mechanisms, corresponding to two different migration mechanism. If two peaks mutually overlapped, then the $I_{\max}(T_{pd})$ plot should exhibit two separate maxima, but the experimental results proved that this is not the case.

Partial heating technique

The powerful partial heating method [10, 31] was also applied in order to estimate the temperature distribution of the activation energy E of the HT peak. As stated in the Theory section, E is identical to the migration enthalpy h^m of the conduction charges. The method consists of successive depolarizations of the mechanism and provides a set of initial rise curves. Whatever the nature of the mechanism is (dipolar or space charge), the initial rise of the

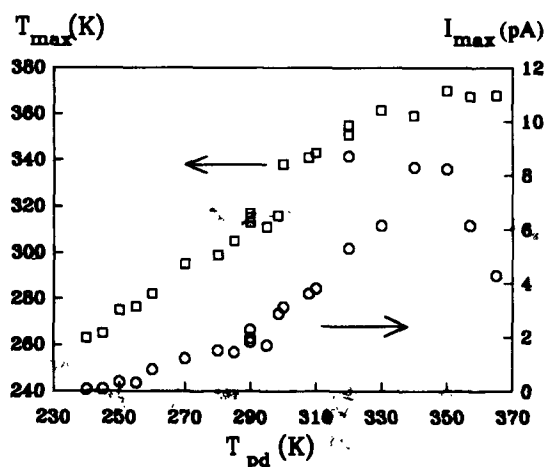


Fig. 8. Maximum temperature T_{\max} and amplitude I_{\max} of components of the HT peak, isolated by employing the selective polarization method, vs polarization (and depolarization) temperature T_{pd} .

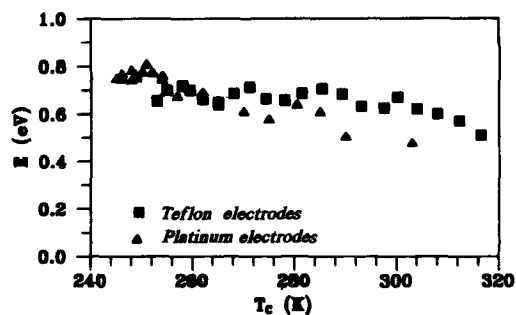


Fig. 9. Temperature distribution of activation energy E evaluated from the initial rise discharge curves (partial heating method). T_c denotes the end temperature of each rise.

thermocurrent directly leads to the accurate evaluation of E via eqn (4). The temperature distribution of E can also show the existence of two or more overlapping mechanisms provided E is distinctly accumulated around to two or more different values. In Fig. 9 we present the evaluated values of E vs the cooling temperature T_c where the recording of the initial rise was ended by abrupt cooling of the specimen. We observe that the experimental points are gathered around the value of 0.70 eV , being distributed from 0.48 to 0.80 eV . The points do not gather around any other activation energy value, supporting the aforementioned result of the selective polarization technique, i.e. that the HT band does not overlap or mask some other peak activated at the temperature region of the HT band.

In the temperature region in which our experiments were performed, the extrinsic vacancy population typically dominates in relation to the intrinsic population. It is probable that cation vacancies are the major vacancies as a result of charge compensation for the introduction of cation impurities. It is expected from the impurity content that small ionic radius impurities (such as K^+ and Na^+) would be mobile enough to participate in the conductivity phenomenon.

CONCLUSIONS

The TSDC method was used to detect and investigate the features of the ionic relaxation of polycrystalline dolomite. The strong HT mechanism is related to the space charge motion and is characterized by the distribution in values of the relaxation time. The selective polarization and partial heating techniques indicated that the HT band manifests itself as a unique free charge relaxation mode. The activation energy values estimated correspond to the free carrier migration enthalpy, establishing the TSDC method as an alternative to the measurement of high temperature conductivity for studying temperature-sensitive materials.

REFERENCES

1. Battey, M. H., *Mineralogy for Students*. Longman, London, 1981.
2. Deer, W. A., Howie, R. A. and Zussman, J., *An Introduction to the Rock Forming Minerals*. Longman, Essex, 1966.
3. Catti, M., Pavese, A., Dovesi, R. and Saunders, V. R., *Phys. Rev. B*, 1993, **47**, 9189.
4. Baysar, A. and Kuester, J. L., *IEEE Trans. Microwave Theory Techniques*, 1992, **40**, 2108.
5. Papathanassiou, A. N., Grammatikakis, J., Katsika, V. and Vassilikou-Dova, A. B., *Radiation Effects Defects Solids*, 1995, **134**, 247.
6. Papathanassiou, A. N., Ph.D. thesis, University of Athens, 1995.
7. Bogris, N. G., Grammatikakis, J. and Papathanassiou, A. N., in *Proceedings of the XII International Conference on Defects in Insulating Materials ICDIM '92*, ed. O. Kanert and J.-M. Spaeth. World Scientific Publishing Singapore, 1993, p. 804.
8. Papathanassiou, A. N. and Grammatikakis, J., *Phys. Rev. B*, 1996, **53**, 16252.
9. Papathanassiou, A. N. and Grammatikakis, J., *Phys. Rev. B*, 1996, **53**, 16247.
10. Papathanassiou, A. N., Grammatikakis, J. and Bogris, N., *Phys. Rev. B*, 1993, **48**, 17715.
11. Suptiz, P. and Teltow, J., *Phys. Stat. Solidi*, 1967, **23**, 9.
12. Philibert, J., *Atom movements, Diffusion and Mass Transport in Solids*. Les Editions de Physique, Paris, 1991.
13. Varotsos, P. and Alexopoulos, K., *J. Phys. Chem. Solids*, 1980, **41**, 443.
14. Varotsos, P. A. and Alexopoulos, K. D., *Thermodynamics of Point Defects and Their Relation with Bulk Properties*, ed. S. Amelinckx, R. Gevers and J. Nihoul. North-Holland, Amsterdam, 1985.
15. Jonscher, A. K., *Dielectric Relaxation in Solids*. Chelsea Dielectrics Press Ltd, London, 1983.
16. Vanderschueren, J. and Gasiot, J., Field induced thermally stimulated currents, in *Thermally Stimulated Relaxation in Solids*, ed. P. Braunlich. Springer-Verlag, Berlin, 1979.
17. Laredo, E., Suarez, N., Bello, A., Puma, M., Figueroa, D. and Schoonman, J., *Phys. Rev. B*, 1985, **32**, 8325.
18. Spinolo, G. and Anselmi-Tamburini, U., *High Temp. High Press.*, 1988, **20**, 109.
19. Spinolo, G. and Anselmi-Tamburini, U., *J. Phys. Chem.*, 1989, **93**, 6837.
20. Lavergne, C. and Lacabanne, C., *IEE Electrical Insulation Mag.*, 1993, **9**, 5.
21. Zielinski, M. and Kryszewski, M., *Phys. Stat. Sol. (a)*, 1977, **42**, 305.
22. Papathanassiou, A. N., Grammatikakis, J. and Bogris, N., *Phys. Rev. B*, 1994, **50**, 14160.
23. Muller, P., *Phys. Stat. Sol. (a)*, 1974, **23**, 165.
24. van Turnhout, J., *Thermally Stimulated Discharge of Polymer Electrets*. Elsevier, Amsterdam, 1975.
25. Schrader, S. and Carius, H.-E., in *Proceedings of the 7th International Symposium in Electrets ISE7*, ed. R. Gerhard-Multhaupt, W. Kunstler, L. Brehmer and R. Danz. IEEE, Berlin, 1991, p.581.
26. van Turnhout, J., Thermally stimulated discharge of polymers, in *Electrets*, ed. G. M. Sessler. Springer-Verlag, Berlin, 1980.
27. Nedetzka, T., Reichle, M., Mayer, A. and Vogel, H., *J. Phys. Chem.*, 1970, **74**, 2652.
28. Zielinski, M. and Kryszewski, M., *J. Electrostatics*, 1977, **3**, 69.
29. McKeever, S. W. S., *Thermoluminescence of Solids*. Cambridge University Press, Cambridge, 1985, pp. 76–80.
30. McKeever, S. W. S., *Phys. Stat. Solidi (a)*, 1980, **62**, 331.
31. Creswell, R. and Perlman, M., *J. Appl. Phys.*, 1970, **41**, 2365.